ENTPD3-specific CAR regulatory T cells for local immune control in T1D

Tom Pieper[1], Tobias Riet[1,2], Valerie Saetzler[1], Katharina Bergerhoff[3], Jenny McGovern[3], Louise Delsing[4], Mark Atkinson[5], Tracey Lodie[3], Lutz Jermutus[6], Fatih Noyan[1], Michael Hust [7], Irina Kusmartseva[5], Maike Hagedorn[1], Maren Lieber[1], Pierre Henschel[1], Viktor Glaser[1], Robert Geffers[8], Mingxing Yang[9], Julia Polansky-Biskup[9], Britta Eiz-Vesper[10], Agnes Bonifacius[10], Marc Martinez Llordella[3], Luke Henry[3], Daniela Penston[3], Artemis Gavriil[3], Thomas Grothier[3], Evanthia Nikolopoulou[3], Nikolaos Demertzis[3], Victoria Koullourou[3], Phillipa Cox[3], Bader Zarrouki[11], Marcella Sini[12], Janice Pfeiff[13], Isabelle Matthiesen[4], Matthias Hardtke-Wolenski[1,14*], Elmar Jaeckel[1,15*]

1 Hannover Medical School, Dept. of Gastroenterology, Hepatology, Infectious Diseases and Endocrinology, Hannover, Germany

2 University of Cologne, University Hospital of Cologne and Center for Molecular Medicine Cologne (CMMC), Department I of Internal Medicine, Tumor Genetics, Cologne, Germany

3 Quell Therapeutics Limited, London, UK

4 Cell & Gene Therapy Safety, Clinical Pharmacology & Safety Science, R&D, AstraZeneca, Gothenburg, Sweden

5 University of Florida, Dept. of Pathology, Immunology and Laboratory Medicine, Gainesville, USA

6 Research and Early Development, Cardiovascular, Renal and Metabolism, BioPharmaceuticals R&D, AstraZeneca, Cambridge, UK

7 Technische Universität Braunschweig, Dept. Medical Biotechnology, Braunschweig, Germany

8 Helmholtz Centre for Infection Research, Genome Analytics, Braunschweig, Germany

9 Berlin Institute of Health Center for Regenerative Therapies at Charité Universitätsmedizin Berlin, and German Rheumatology Research Centre, Immuno-Epigenetics, Berlin, Germany

10 Hannover Medical School, Institute of Transfusion Medicine and Transplant Engineering, Hannover, Germany

11 Bioscience Metabolism, Research and Early Development, Cardiovascular, Renal and Metabolism (CVRM), BioPharmaceuticals R&D, AstraZeneca, Gothenburg, Sweden

12 Discovery Imaging IBA, Clinical Pharmacology & Safety Science, R&D, AstraZeneca, Gothenburg, Sweden

13 Department of Pathology, Clinical Pharmacology & Safety Sciences, R&D, AstraZeneca, Gothenburg, Sweden

35 14 University of Duisburg-Essen, University Hospital Essen, Institute of Medical Microbiology,
36 Essen, Germany

37 15 University of Toronto, Center for Liver Transplantation, Center for Islet Transplantation,
38 Multi Organ Transplant Center, Toronto, Canada

39 *contributed equally

Abstract

Despite advances in Type 1 Diabetes (T1D) management such as hybrid closed loop systems, patients still face significant morbidity, reduced life expectancy, and impaired glucose regulation compared to healthy individuals or those with pancreas transplants.

Here we developed beta cell-specific Chimeric Antigen Receptors (CAR) targeting the antigen ectonucleoside triphosphate diphosphohydrolase 3 (ENTPD3) using a novel cell-based phage display methodology. ENTPD3 is highly expressed on beta cells of both early and progressed T1D patients. ENTPD3 CAR regulatory T cells (Tregs) homed, expanded and persisted in pancreatic islets in a T1D mouse model (NOD) and completely prevented disease progression. Human ENTPD3 CAR Tregs displayed a stable regulatory phenotype, strong activation, and suppression. Importantly, ENTPD3 CAR T cells recognised and were fully activated by human islets.

This approach holds great promise as a durable treatment option for patients with prediabetes, new-onset diabetes, or those undergoing beta cell replacement therapy.

54 **Introduction:**

55 Patients diagnosed with Type 1 Diabetes (T1D) continue to face substantial challenges,
56 experiencing significant morbidity primarily attributable to the complications arising from
57 fluctuating blood glucose levels and overall see a reduction in life expectancy by a decade[1-3].

58 Although technological advancements, such as Continuous Glucose Monitoring (CGM) sensors
59 and hybrid closed-loop pumps, have improved glycaemic control, particularly during nocturnal
60 periods, they fail to replicate the robust metabolic control achieved by endogenous beta
61 cells[4,5].

62 While pancreas, islet or stem cell derived beta cell transplantation offers a potential biological
63 replacement for beta cells, the associated challenges and risks, including immune rejection
64 and the need for systemic immunosuppression, underscore the demand for innovative
65 therapeutic approaches[6].

66 Disease modifying therapies and immune modulation strategies, particularly in the context of
67 new-onset T1D, have recently demonstrated success in clinical trials, albeit leading to only
68 transient preservation of minimally stimulated c-peptide responses[7,8].

69 Clinical trials administering polyclonal regulatory T cells (Tregs) in patients with T1D have
70 shown a good safety profile but limited efficacy[9,10]. Pre-clinical data has shown superiority of
71 antigen-specific Tregs over polyclonal Tregs in the NOD model of T1D and Tregs with beta cell-
72 specific T cell receptors (TCR) have shown promise in establishing prolonged local tolerance in
73 pre-clinical models[11-13] but challenges arising from Major Histocompatibility Complex II (MHC
74 II) polymorphism and the heterogeneity of immune responses in T1D patients have hindered
75 the development of a viable clinical product for over two decades.

76 Recent advancements in the use of Chimeric Antigen Receptor (CAR) Treg cells have
77 demonstrated success in achieving local immune control in murine and humanized mouse
78 models. MHC I A*02 specific CAR-Tregs, activated independently of MHC II restriction, exhibit
79 localized accumulation and prevented allograft rejection in mouse models and humanized
80 mice[14-16]. Ongoing clinical trials exploring the use of A2-CAR-Tregs in kidney and liver
81 transplantation provide a foundation for extending this approach to the context of T1D.

82 Herein, we identified ectonucleoside triphosphate diphosphohydrolase 3 (ENTPD3) as beta
83 cell specific target and generated CARs directed against ENTPD3 using a novel phage display
84 approach. We provide evidence for the antigen-specific functionality and safety of ENTDP3
85 CAR-Tregs *in vivo*, *in vitro* and *ex vivo*. Thus, ENTPD3-specific CAR Tregs offer a potential avenue
86 for achieving durable, targeted and pancreas-specific immune control in patients with T1D.

87 **Results:**

88 **ENTPD3 as a Potential Target for Islet-Specific CAR-Treg Therapies**

89 Previous attempts to develop CAR therapies targeting insulin, the most specific protein
90 associated with beta cells, were ineffective in preventing or treating T1D[17]. In silico research
91 suggested that ENTPD3, a surface protein, is highly expressed in both mouse and human beta
92 cells[18-20].

93 It is critical for potential therapeutic targets to be expressed at all stages of T1D
94 pathophysiology. We demonstrated by histological analysis of pancreatic samples from
95 patients at various stages of T1D, obtained through the nPOD (Network for Pancreatic Organ
96 Donors with Diabetes) consortium, that ENTPD3 is consistently co-expressed with insulin
97 across multiple stages of disease, from the autoantibody-positive stage to stage 3 (Fig. 1AB).
98 Notably, some expression was detected in non-beta cells, during established, long duration
99 T1D (Fig. 1A).

100 The protein expression of ENTPD3 was corroborated by re-analysis of single-cell RNA
101 sequencing data from patients at different stages of T1D (Fig. 1C-E)[21], showing strong
102 expression in beta cells across both autoantibody-positive and overt T1D stages as well as in
103 delta cells as well. We confirmed specific expression of ENTPD3 protein in human pancreatic
104 islets by immunohistochemistry analysis of a wide panel of human tissues (Fig. 1F). Finally, we
105 confirmed that in prediabetic and diabetic NOD mice, ENTPD3 was expressed in islets, with
106 minimal expression detected in surrounding ductal cells (Fig. 1G). These findings indicate that
107 the NOD mouse model is suitable for proof-of-concept testing of ENTPD3-targeted CAR-Tregs.

108 **Generation of ENTPD3-Specific Single-Chain Variable Fragment (scFv) Binders via Protein-**
109 **Cell Based Phage Display**

110 Traditionally, CAR therapies have relied on a limited number of established monoclonal
111 antibodies[22]. In contrast, our approach sought to generate diverse scFv binders and assess
112 their functional properties. By employing human phage display libraries, we expedited the
113 translation of binders into human CARs for clinical trials without requiring murine-to-human
114 adaptation. Previous work from this lab demonstrated that successful panning against human
115 peptide sequences can result in the selection of binders that cannot recognise intact proteins
116 on cell surfaces [23]. Consequently, we developed an assay that enriched scFv-phage binders
117 against correctly folded surface proteins on target cells (Suppl. Fig. 1A) using cell sorting
118 following rigorous pre-absorption and washing (Suppl. Fig. 2). This method produced a diverse
119 array of ENTPD3-specific binders (Fig. 2A).

120 We confirmed binding specificity using intact cells expressing ENTPD3 on the cell surface (Fig.
121 2BC). Furthermore, murine ENTPD3-specific binders were shown to stain islets of C57Bl/6
122 mice, confirming that selected binders could recognise ENTPD3 in the pancreas (Fig. 2D).

123 Interestingly, we were unable to identify binders that cross-reacted with human and murine
124 ENTPD3 (Fig. 2BC), which is likely attributed to the low sequence homology between the
125 human and murine extracellular domains (Suppl. Fig. 1B). Therefore, we continued with
126 different scFvs for either murine-specific ENTPD3 to perform proof-of-concept experiments in
127 NOD mice or human-specific ENTPD3 to further characterise of human CAR Tregs,
128 respectively.

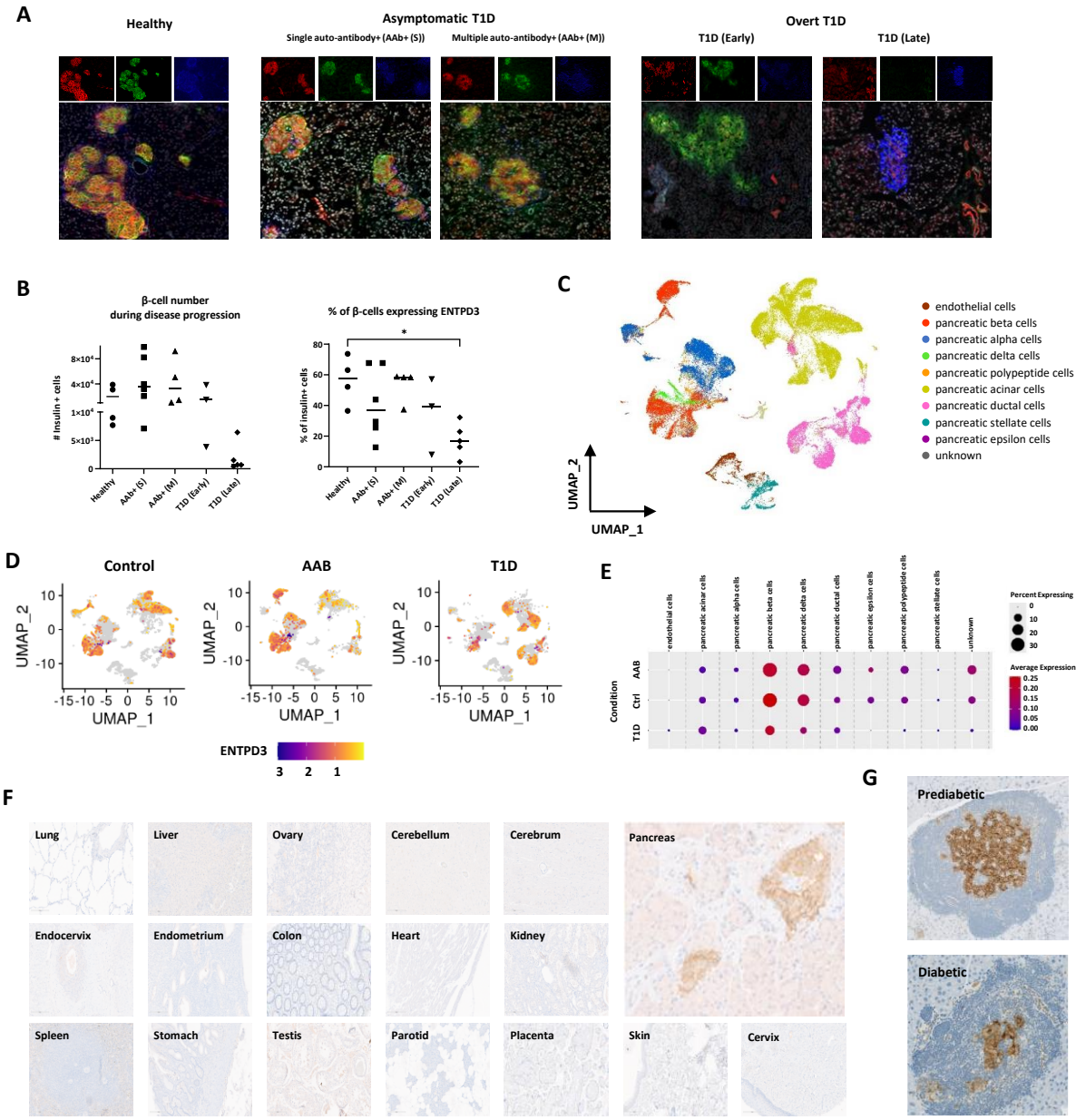

Figure 1: *ENTPD3 as potential target for islets-specific CAR-Treg therapies* **(A)** Human pancreatic sections (nPOD) of individuals with different disease progression (Single Autoantibody positive: AAb+ (S); Multiple Autoantibody positive: AAb+ (M); Early and late T1D) were stained with anti-ENTPD3 antibody (red). Insulin (green) and glucagon (blue) were co-stained. Non-diabetic sample served as control. **(B)** Quantification of islets staining for ENTPD3. Left: Number of beta cells (Insulin+). Right: Percentage of beta cells expressing ENTPD3. n per condition = 3-6. **(C-E)** ENTPD3 expression of human pancreatic cells of nPOD samples. **(C)** UMAP visualization of cellular clusters of human pancreatic islets. (D) UMAP visualizations of ENTPD3 expression in islets cells of healthy (Control), autoantibody-positive (AAB) and T1D individuals (T1D). **(E)** Quantification of D. Dot size resembling percent of cells expressing ENTPD3 within cell cluster. Colours indicating average expression strength. **(F)** Tissue micro array (TMA) of different human organs stained for ENTPD3 (brown) show that membranous ENTPD3 expression is highly specific to pancreatic islets. Hematoxylin counterstain in blue. **(G)** Pancreatic sections of prediabetic and diabetic NOD mice were stained for ENTPD3 (brown) and counterstained with hematoxylin (blue).

To rule out cross-reactivity with other membrane proteins, we screened the selected binders against 5,500 human membrane proteins using a membrane proteome array, confirming exclusive binding to ENTPD3 without cross-recognition of ENTPD1 or ENTPD2 (Fig. 2EF). ENTPD3 is an ectonucleotidase involved in extracellular nucleotide and ATP hydrolysis and thereby in purinergic signalling, contributing to the regulation of insulin secretion[19,24]. Consequently, it was essential to demonstrate that our scFv binders did not interfere with ENTPD3 enzymatic activity. We observed no evidence that scFv binding impaired ENTPD3 function, even when added at high concentrations (Fig. 2GH).

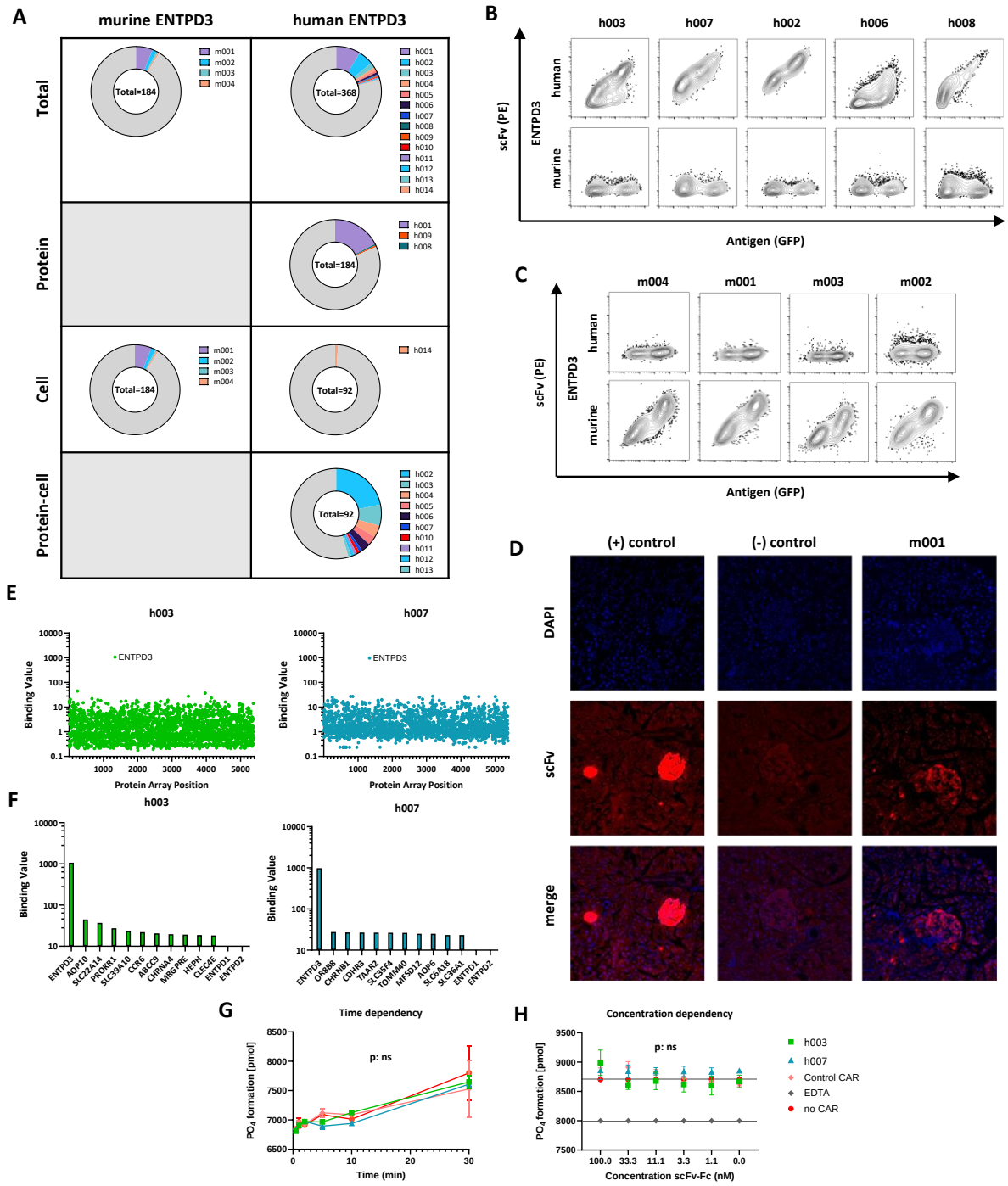

Figure 2: *Generation of ENTPD3-specific scFv binders by protein- and cell-based phage display* **(A)** Outcome of scFv binders by different panning strategies for murine ENTPD3 and human ENTPD3. Total number of analysed scFv binders per strategy are given in the centre of each plot. Proportions of unique scFv clones (color-coded) and non- and unspecific binders (grey). **(B-C)** Binding of human **(B)** and murine **(C)** ENTPD3-specific scFv binders was measured by flow cytometry on human or murine ENTPD3 expressing HEK293T cells, respectively. ENTPD3 expression on HEK cells was reported by coexpression of eGFP. Representative plots of selected binders. **(D)** Staining of C57BL/6 pancreatic sections by murine ENTPD3-specific binder m001. Insulin-specific FITC-conjugated antibody was used as positive control (left). Incubation with scFv m001 was followed by FITC-conjugated secondary antibody (right). Staining only secondary antibody served as negative control (middle). **(E)** Membrane Proteome Array (MPA) screening was performed by testing of human ENTPD3 binders. Binding values are given for clones h003 and h007 in an scFv-Fc format for 5,372 distinct human membrane protein clones. **(F)** Binding values of MPA for ENTPD3 and 10 following proteins with highest values and ENTPD1 and ENTPD2. **(G-H)** ENTPD3 enzymatic activity in the presence of soluble ENTPD3, ADP and scFv-Fc of h003 or h007. ENTPD3 activity (PO_4 formation) was measured by malachite green phosphate assay. Measured in triplicates. **(G)** Phosphate formation up top 30 min after incubation with 3.3 nM ENTPD3-specific scFv-Fc. No CAR and control CAR served as control. (H) Phosphate formation after incubation with varying concentrations (100 – 1 nM) of ENTPD3-specific scFv-Fc. Additionally, incubation with EDTA served as positive control for ENTPD3 inhibition. Data are presented as mean ± SD of triplicates. p values determined by two-way ANOVA of h003, h007 and Control CAR conditions, respectively. ns: $P > 0.05$.

164 **Murine ENTPD3-Specific CARs are Activated upon Target Engagement and Prevent**
165 **Cyclophosphamide-Induced Diabetes *In Vivo***

166 Murine ENTPD3-specific CARs were constructed using either CD8 hinge/transmembrane
167 domains or IgG hinge/CD4 transmembrane domains, the latter featuring a mutated Fc
168 receptor binding region to prevent nonspecific activation (Fig. 3AB). These second-generation
169 CARs include a CD3zeta activation domain and a CD28 costimulatory domain, which are
170 optimal for Treg activation, as demonstrated by Levings and colleagues[25]. CARs were tested in
171 T cell hybridomas where NFAT activation induced eGFP expression via a minimal IL2 promoter
172 (Suppl. Fig. 3A). CAR candidate m001 exhibited strong target-specific activation without
173 background signalling in both hinge formats (Fig. 3CD) and was not stimulated by the human
174 ENTPD1 (Suppl. Fig. 3B). m001 also recognised MIN6 beta cells (Suppl. Fig. 3CD) which were
175 shown previously to express low levels of ENTPD3[19]. In murine CD4+ T cells, ENTPD3-specific
176 CARs stimulated target-dependent proliferation and activation (Fig. 3E, Suppl. Fig. 4AB).

177 In a spontaneous diabetes NOD model, in which disease was synchronised by a single low-
178 dose cyclophosphamide injection, ENTPD3-specific CAR-T cells (m001) showed strong early
179 homing to pancreatic islets (day 3), unlike PE-specific control CAR-T cells (Fig. 3FG). In contrast,
180 ENTPD3-specific CAR-T cells (m001) were absent in pancreatic lymph nodes. After 21 days,
181 15% of CD4+ cells in the pancreatic islets were ENTPD3 CAR-Tregs, reflecting a combination of
182 homing, expansion, and persistence (Suppl. Fig. 4C).

183 In the cyclophosphamide-induced T1D model (Fig. 3H), m001 CAR-Tregs prevented diabetes
184 onset, with no cases of T1D in the treatment group, compared to 50% incidence in control
185 animals (Fig. 3I). In this experiment, we confirmed that ENTPD3 CAR-Tregs persisted long-term
186 and were exclusively located in pancreatic islets (Fig. 3J). We observed no detectable homing
187 to off-target tissues such as the testes or colon, as confirmed by digital PCR (Fig. 3K). Finally,
188 murine ENTPD3 CAR-Tregs displayed a stable regulatory phenotype (Suppl. Fig. 5).

189 **Generation of Human CARs Recognising ENTPD3**

190 We deployed scFvs recognizing human ENTPD3 (Fig. 2B) to construct human CARs featuring
191 either CD8 hinge and CD8 transmembrane region and performed functional characterization
192 in Jurkat cells expressing luciferase under an NFAT-dependent minimal IL-2 promoter. Five
193 CARs were identified that exhibited strong activation with no tonic signalling in the absence
194 of antigen (Fig. 4A). Notably, CARs were also capable of recognising ENTPD3 on RT-4 cells,
195 which endogenously express low levels of ENTPD3.

196 The five CARs identified in the screening stage were transduced into human nTregs. In
197 activation assays using these cells, we observed robust upregulation of activation markers
198 CD69, CD137, and the Treg-specific marker GARP following activation by ENTPD3 (Fig. 4B-D),
199 with activation comparable to that of TCR stimulation. Coculture experiments of ENTPD3
200 expressing B cells, allospecific T effector cells (Teff) and ENTPD3 CAR Tregs demonstrated that
201 ENTPD3 CAR Tregs could be activated by B cells expressing ENTPD3 to cross-suppress CD4+
202 Teffs activated by a TCR driven response to allogeneic B cells. This ability to control T cells with
203 different specificities is a crucial function of CAR-Tregs given the need to suppress T cells
204 reactivity against various beta cell antigens within the islets (Fig. 4E). Importantly, CAR
205 transduction did not affect the stability of the regulatory phenotype, as evidenced by
206 sustained expression of CD25, FOXP3, CTLA-4, Helios and ICOS as shown for CAR candidates
207 h003 and h007 (Fig. 4F).

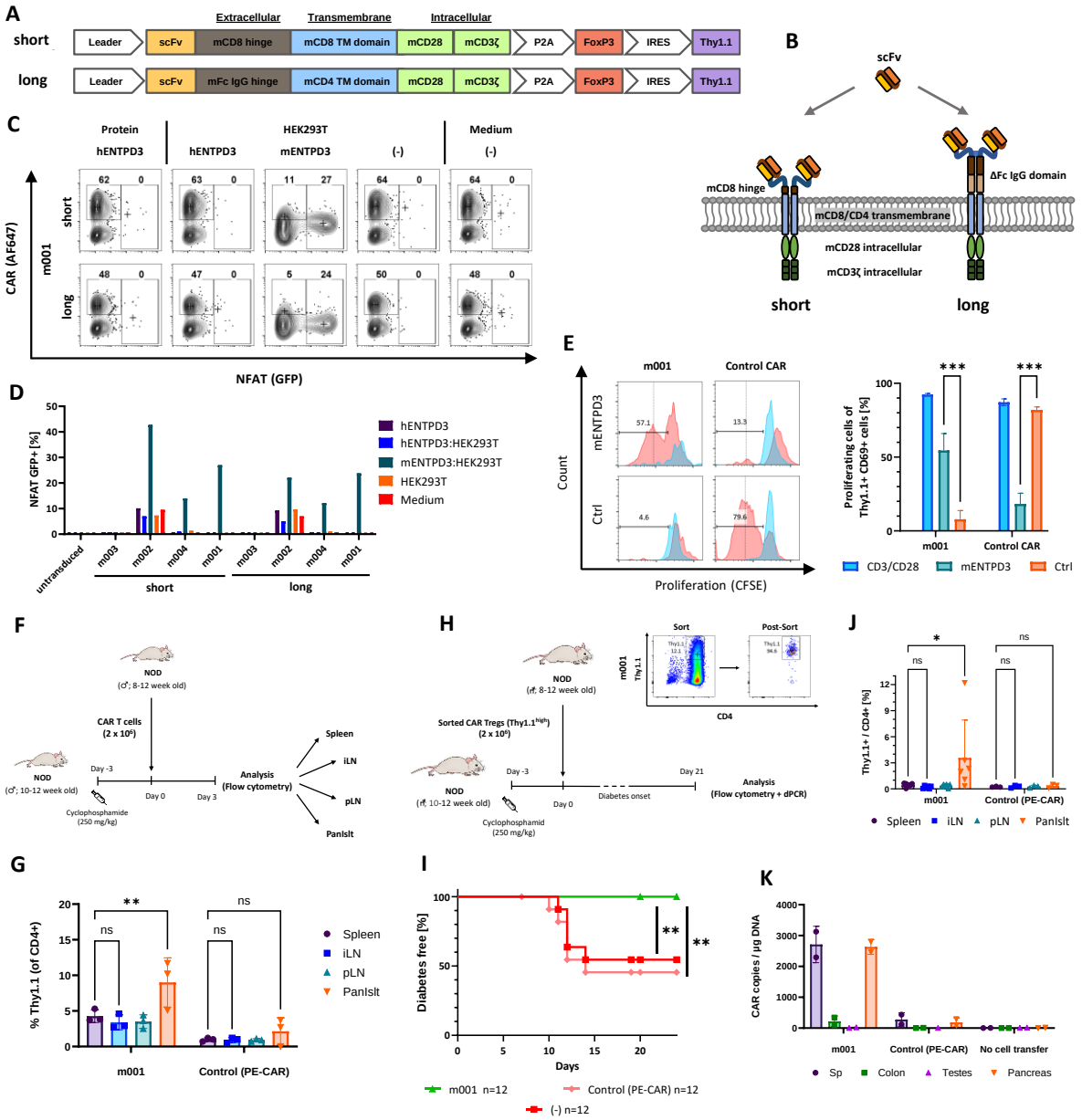

Figure 3: *Murine ENTPD3-specific CAR are functionally stimulated upon target contact and prevent cyclophosphamide-induced diabetes in vivo* **(A)** Design of murine CD8-derived hinge CARs (short) and Fc-IgG-derived hinge CARs (long), containing a FOXP3 expression cassette separated by P2A cleavage side, and reporter gene Thy1.1 (CD90.1) under control of an IRES. **(B)** Illustration of both CAR constructs as expressed on the cell surface. **(C)** Representative plots of stimulation of m001 in short and long hinge CAR format, respectively, in NFAT-GFP reporter cell line. CAR stimulation shown as NFAT-controlled GFP expression and CAR expression shown as anti-Fab antibody AF647 staining. **(D)** Screening of further murine ENTPD-specific candidates for CAR stimulation in the aforementioned system. **(E)** Proliferation of CAR T cells measured as dilution of CFSE signal. CFSE labelled murine CD4+ CAR T cells (mL-m001 or Control (PE-specific) CAR) were stimulated on mENTPD3 or control antigen PE, or by aCD3/CD28 bead stimulus. Counts normalized to mode. Red: Stimulated CAR T cells (of CD69+ Thy1.1+). Blue: Unstimulated cells (of CD69- Thy1.1-). Left: Representative histograms. Right: Quantification of % Proliferation of stimulated CAR T cells (of CD69+ Thy1.1+). Mean ± SD, triplicates. p values determined by two-way ANOVA and multiple comparison testing (Tukey's test). **(F)** Schematic overview of setup for CAR T cell homing experiment in NOD mice. **(G)** Comparison of biodistribution of m001 and Control (PE-specific) CAR Teffs. CD4+ populations were analysed for percentage of Thy1.1+ cells. Data are presented as mean ± SD. n=3 per group. p values determined by two-way ANOVA and multiple comparison testing (Tukey's test). **(H)** Schematic overview of experimental setup for prevention of cyclophosphamide-induced diabetes in NOD mice. **(I)** Diabetes-free individuals over the course of the experiment. n=12 per group. Data from 8 independent experiments. p value determined by log-rank test for m001 CAR cTreg compared to Control (PE-specific) CAR cTreg and cyclophosphamide-only treated animals. **(J)** Comparison of biodistribution of m001 CAR-cTregs and Control (PE-specific) CAR cTregs at experimental endpoints (n = 3-6 per group). Data are presented as mean ± SD of Thy1.1+ in the CD4+ population. p values determined by two-way ANOVA and multiple comparison testing (Tukey's test). **(K)** Biodistribution of m001 CAR Tregs in ENTPD3-expressing tissues by digital PCR. Organs of two mice per group were saved at experimental endpoints and total gDNA was analysed by digital PCR. Copy numbers of CAR Treg-specific WPRE sequence per µg gDNA are displayed. P values for all experiments * P < 0.033, ** P < 0.002, *** P < 0.001.

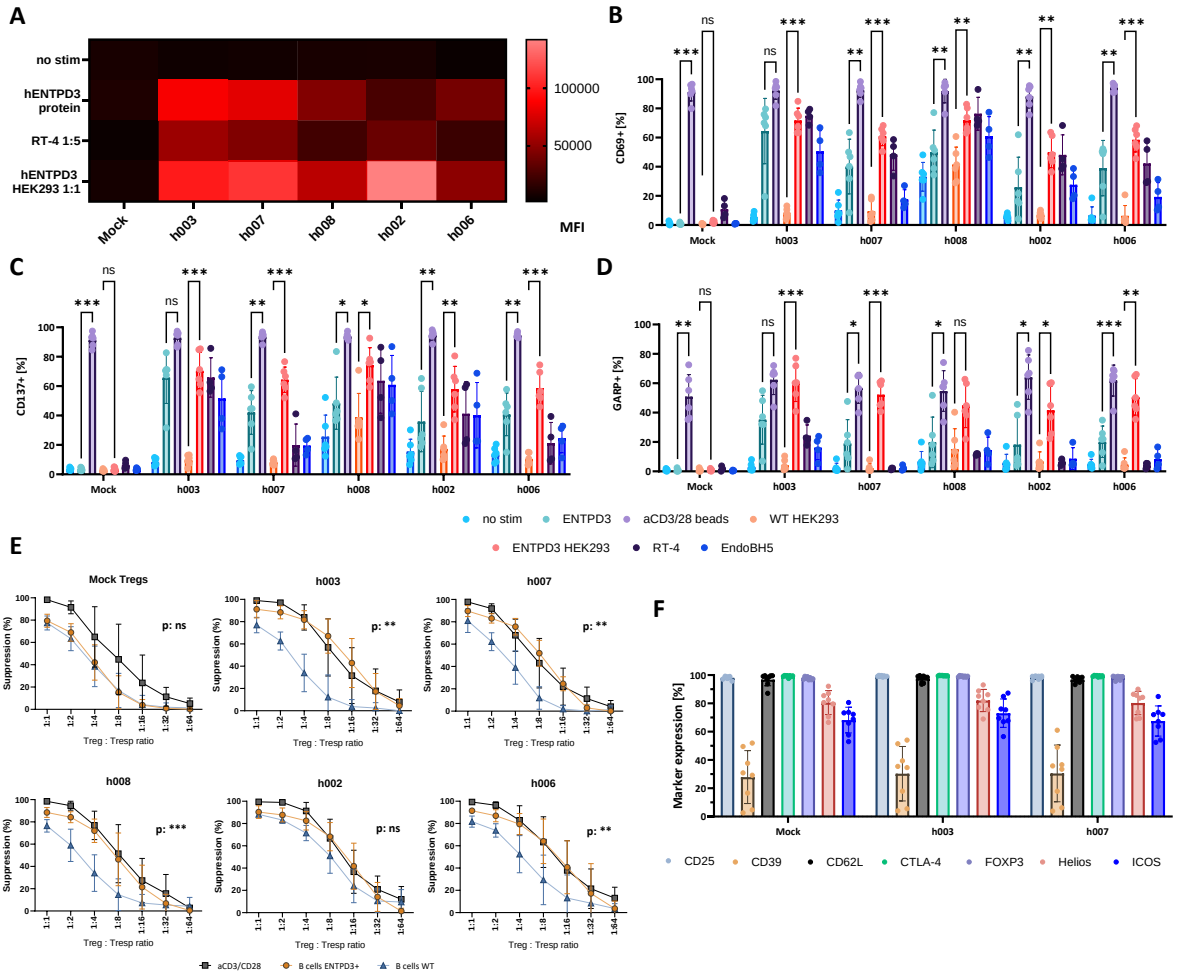

Figure 4: *Human ENTPD3-specific CAR Tregs are functional and maintain Treg phenotype and suppressive function* **(A)** NFAT luciferase Jurkat cell line was transduced with CARs comprising different human ENTPD3-specific scFv (h003, h007, h008, h002 and h006). After 5 days cells were activated with human ENTPD3 extracellular domain peptide, cell lines expressing ENTPD3 (RT-4 and ENTPD3.HEK293T) at indicated ratios or left unstimulated. Activation of cells was determined by luminescence measurement. Heatmap shows relative activation levels in response to stimulus. Black represents the lowest levels of activation with red/pink showing highest levels of activation. Representative of 3 separate experiments. **(B-D)** Human ENTPD3 CAR Tregs were co-cultured with ENTPD3 extracellular domain, ENTPD3 expressing HEK293T cells, RT-4, EndoBH5 cells or controls (aCD3/aCD28 beads, WT HEK293T and no stimulation). After 24h activation markers CD69 **(B)**, CD137 **(C)** and GARP **(D)** were assessed by flow cytometry. Mean ± SD of n=6 donors. p values determined by two-way ANOVA and multiple comparison testing (Tukey's test). **(E)** CAR Tregs were co-cultured with WT B cell line, ENTPD3 expressing B cell line or aCD3/28 beads and decreasing numbers of CTV-labelled CD4+ Teffs for 5 days. Cells were assayed by flow cytometry and proliferation of Teffs was determined by CTV dilution. Graphs show percentage suppression by ENTPD3 CARs and mock transduced cells. Percentage suppression was calculated by normalizing proliferation of Teffs stimulated in the presence of Tregs to Teffs alone. Data are presented as mean ± SD of n=4-5 donors. p values determined by two-way ANOVA of B cells ENTPD3 and B cells WT conditions, respectively. **(F)** h003 and h007 CAR Tregs were collected and stained by flow cytometry for indicated markers. Percentage of each marker shown from the total CD4 population for Mock Tregs or gated on CAR+ cells for the CAR Tregs. Mean ± SD of n=8 donors. P values for all experiments * P < 0.033, ** P < 0.002, *** P < 0.001.

Second-generation CARs utilise partial activation motifs of the TCR complex, yet provide CD28 costimulatory signals. Therefore, we compared human ENTDP3-specific CAR Tregs in terms of CAR or TCR-based stimulation, focusing on the promising CAR candidate h003 more closely. CAR stimulated h003 CAR Tregs produced comparable levels of IL-10, IL-8, and IL-17a to those observed after TCR activation, with significantly increased TGF-β production (Fig. 5B). CAR Treg phenotype was stable after both CAR and TCR stimulation indicative of high FOXP3 and CTLA4 expression, and activation marker GARP was upregulated (Fig. 5C). Epigenetic demethylation of the TSDR region remained stable and indiscernible from untouched nTregs, further confirming phenotypic stability (Fig. 5D)[26]. We further investigated the molecular signalling pathways in CAR Tregs by RNA sequencing after CAR- and TCR-based activation. Interestingly, critical Treg-associated genes, such as CD25, GARP, ICOS, and CTLA4, displayed similar activation patterns, whereas LAG3, PD1 and TIGIT were more highly expressed after

CAR activation (Fig. 5E). While most genes were similarly regulated following TCR and CAR stimulation, comparative cluster analysis identified genes that were uniquely upregulated following CAR stimulation in cluster 2 (Fig. 5F), characterised by genes involved in IL-2 signalling and NF-kB activation (Fig. 5G) and genes related to negative regulation of immune cells (Suppl. Fig. 6). Additionally, subtle differences in gene expression emerged as indicated by pairwise comparison (Fig. 5H).

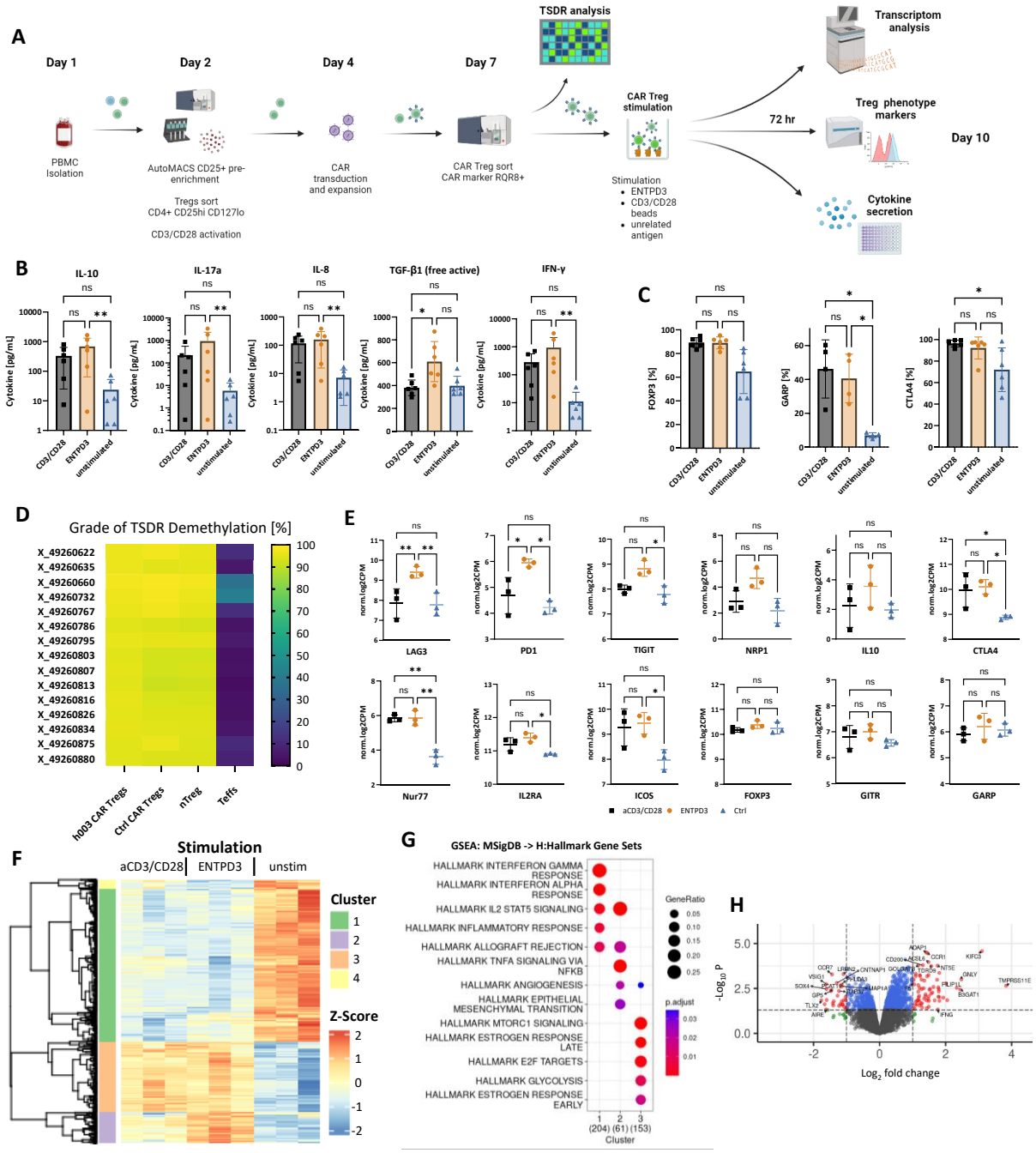

Figure 5. *ENTPD3 CAR Tregs (candidate h003) maintain Treg-specific phenotype and gene expression upon stimulation* **(A)** Schematic overview and design of human CAR Treg stimulation assay containing TSDR, transcriptomics and phenotype markers and cytokine secretion readouts for testing of CAR h003. **(B)** Treg cytokine profile upon CAR and TCR-dependent stimulation. ENTPD3 CAR Treg cells were incubated with ENTPD3, PE (control antigen) or aCD3/CD28 beads. Cytokine concentration was determined by cytokine bead array. Data are presented as mean ± SD of n=6 donors. p values determined by two-way ANOVA and multiple comparison testing (Tukey's test). **(C)** Expression of Treg phenotype and activation markers FOXP3, GARP and CTLA4 upon stimulation measured by flow cytometry. ENTPD3-specific h003 CAR Tregs stimulated by aCD3/CD28 beads (black), ENTPD3 (orange) or unrelated control antigen (blue). Data presented as mean ± SD of 4-6 donors. p values determined by two-way ANOVA and multiple comparison testing (Tukey's test). **(D)** Analysis of demethylation status of Treg-specific demethylated regions (TSDR). Percentage of demethylation of different TSDRs is shown for ENTPD3 CAR Tregs (h003), Control (PE-specific) CAR Tregs, nTregs and Teffs. Mean of data from 3 donors. **(E)** Gene expression of Treg phenotype and activation genes upon stimulation of

h003 CAR Tregs measured by RNA Sequencing. Black: TCR-dependent stimulation by aCD3/CD28 beads. Orange: CAR-specific stimulation by ENTPD3. Blue: Unrelated control antigen. Data mean ± SD of 3 donors. p values determined by two-way ANOVA and multiple comparison testing (Tukey's test). **(F)** Cluster analysis of transcriptome data. Z-score (color coded) shown for TCR-dependent stimulation by aCD3/CD28 beads, CAR-specific stimulation by ENTPD3 and unstimulated (unrelated control antigen). Data of 3 donors per condition. **(G)** Analysis of Human Molecular Signatures Database (MSigDB) Hallmark gene sets of major clusters 1, 2 and 3. Size of dots represent ratio of represented genes within each cluster. P value is color coded. **(H)** Volcano plot of differentially expressed genes in pairwise comparison of CAR- (ENTPD3) and TCR- (aCD3/CD28 beads) specific stimulation. p values for all experiments * $P < 0.033$, ** $P < 0.002$, *** $P < 0.001$.

Ex vivo Validation of Human ENTPD3 CAR Engagement and Activation

Based on these functional characteristics, three CAR candidates were selected for subsequent testing against human islets. Given the semi-quantitative nature of *in vitro* Treg function assays, we further characterised ENTPD3 CARs in Teffs, as quantitative differences in *in vitro* activation may correlate with variations in *in vivo* activity[27]. Notably, human CD4+ and CD8+ T cells transduced with the ENTPD3 CAR exhibited strong antigen-specific activation and proliferation (Suppl. Fig. 7)

As no relevant humanised T1D animal model exists, we were unable to test human ENTPD3 CAR Tregs *in vivo*. Instead, we assessed the capacity of ENTPD3 CAR-T cells to detect and interact with reaggregated human islets[28] (Fig. 6A), comparing them to preproinsulin-specific CD8+ T cells[29] and HLA-A*02-specific CAR T cells. ENTPD3 CAR T cells displayed time-dependent accumulation and invasion into the islets (Fig. 6B), leading to robust activation indicated by TNF-α and IFN-γ production and near-total destruction of beta cells and their function (Fig. 6CD). Remarkably, ENTPD3 CAR T cells exhibited stronger activation than did preproinsulin-specific CD8+ T cells and A2-specific CAR T cells. These experiments demonstrate that the amount of ENTPD3 on human beta cells and the signal transduction of ENTPD3 CARs are sufficient to activate T cells to full effector functionality.

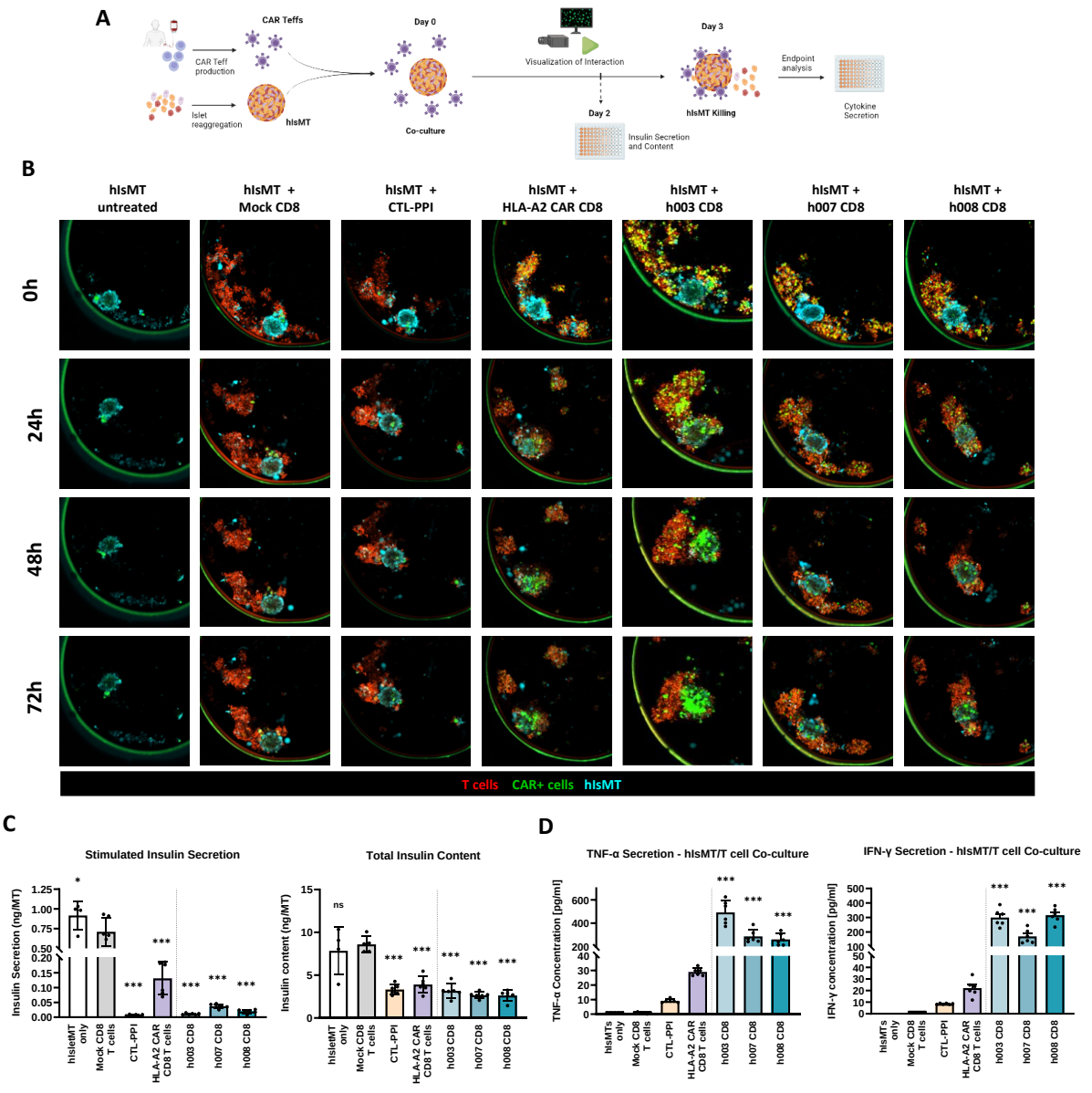

Figure 6: *ENTPD3 CARs interact with human islets micro tissue (hIsMT) spheroids* **(A)** Schematic assay setup. **(B)** Human CD8+ T cells expressing either ENTPD3 CARs (h003, h007 or h008) or HLA-A2 CAR, and GFP reporter cassette were co-cultured with hIsMT spheroids for live imaging. Images show the hIsMT alone, with non-transduced CD8 T cells (Mock), preproinsulin (PPI) specific cytotoxic lymphocytes (CTLs) or CD8 T cells expressing HLA-A2 CAR or ENTPD3 CARs h003, h007 or h008 for timepoints 0, 24, 48 and 72 h. T cells are shown in red, CAR expression is shown in green and hIsMT are stained cyan. **(C)** After 48 h samples of co-cultures were lysed and stimulated insulin secretion (left) and total content (right) was determined by ELISA. Individual dots are technical replicates. Bars represent mean ± SD of n=4-6 **(D)** After 72 h supernatants were collected and assayed for IFN-γ (left) and TNF-α (right). Individual dots are technical replicates. Bars represent mean ± SD of n=6. p values determined by One-way ANOVA with Dunnett's multiple comparisons test comparing all conditions to mock CD8 T cells. Outliers were detected with ROUT's outlier test (Q=5%). *p < 0.05, **p < 0.01, ***p < 0.001.

309 **Discussion:**

310 Polyclonal regulatory T cell (Treg) therapies have demonstrated both safety and phenotypic
311 stability in clinical trials targeting type 1 diabetes (T1D) and after organ transplantation[9,10,30].
312 Despite their excellent safety profiles, these therapies lack efficacy. It is estimated that just
313 one in a million Treg cells will have specificity for a given MHC/self-peptide complex[31].

314 In contrast, studies conducted over the past two decades have highlighted that Tregs
315 recognizing beta cell antigens via their T cell receptors (TCRs), exhibit substantially higher
316 potency than their polyclonal counterparts. Such antigen-specific Tregs have demonstrated
317 long-lasting local immune regulation, successfully reversing even new-onset T1D in murine
318 models[11-13]. Despite these promising results, translating antigen-specific Treg therapy into
319 clinical practice has been hampered by the major histocompatibility complex class II (MHC II)
320 restriction of TCRs, which significantly limits their applicability across diverse patient
321 populations.

322 The advent of chimeric antigen receptors (CARs), which enable MHC-independent antigen
323 recognition, has revolutionized immunotherapy in oncology[22,27]. The successful
324 implementation of CAR T cells in oncology has paved the way for adapting this technology to
325 Tregs to achieve local immune modulation in autoimmune diseases and transplantation. CAR
326 Tregs, targeting mismatched HLA-A*02 molecules, have shown promise in inducing local
327 immune control in transplantation models without systemic immunosuppression[14-16].
328 Encouragingly, these findings have led to clinical trials evaluating CAR Tregs in kidney and liver
329 transplantation (LIBERATE NCT05234190).

330 In our study, ENTPD3 emerged as a highly promising target for beta cell-specific CAR Tregs.
331 ENTPD3 is robustly expressed robustly in pancreatic beta cells and persists across all stages of
332 T1D, from healthy individuals to patients with autoantibodies and recent-onset T1D.
333 Importantly, ENTPD3 is also expressed in delta cells, even in cases of long-standing T1D,
334 suggesting a broad yet specific expression pattern suitable for targeted immune regulation.

335 While current CAR approaches use binders derived from monoclonal antibodies, we employed
336 the phage display technology to generate a large variety of scFv binders. While we and others
337 have shown that scFv generated by phage display can be efficiently used in CAR
338 studies[15,17,23,32,33], these approaches deployed peptides and recombinant proteins which
339 neglects the fact that most CARs target conformational epitopes on cell surface molecules.
340 Therefore, we established a novel phage display approach directly on cells expressing ENTPD3,
341 to generate a large variety of scFv binders recognising the correctly folded target on cells. This
342 enabled us to choose the best binder for Treg activation and suppressive function. The use of
343 human phage display libraries obviated the need for humanisation of CAR constructs,
344 streamlining the translational process.

345 Off-target or on-target/off-tumor effects remain a significant concern in CAR T cell therapies,
346 in immune oncology, where unintended tissue recognition can result in severe toxicities[34,35].
347 These toxicities are unlikely in Treg cell therapies; large doses of polyclonal Tregs have been
348 shown to exhibit a strong safety profile, supporting the low risk associated with CAR Treg
349 therapies[9,10,30].Moreover, restricted expression of ENTPD3 in pancreatic islets, the absence of
350 proinflammatory capabilities in Tregs and their dependency on local interleukin-2 (IL-2) signals
351 at immune activation sites minimise the risk of adverse outcomes.

352 Comprehensive analyses, including tissue microarrays and membrane proteome profiling,
353 confirmed that membranous ENTPD3 expression is restricted to the pancreas. Our
354 investigations further demonstrated that ENTPD3 CARs do not inhibit the enzymatic activity
355 of ENTPD3, mitigating potential unintended consequences of CAR binding on purinergic
356 metabolism and signalling.

357 Although low ENTPD3 mRNA levels were detected in certain tissues, such as the testes and
358 colon, these findings did not translate to protein expression, as confirmed by tissue microarray
359 and in vivo biodistribution studies. ENTPD3 CAR Tregs predominantly localised to pancreatic
360 islets and the spleen, with negligible signals detected in other tissues. Importantly, ENTPD3
361 CAR Tregs accounted for 15% of the CD4+ cells within pancreatic islets, underscoring their
362 strong target tissue homing.

363 Mechanistically, ENTPD3 CAR Tregs differ from TCR Tregs in their mode of action. While TCR
364 Tregs rely on interactions with MHC II and antigen-presenting cells, CAR Tregs act directly
365 within the target tissue. This distinction accounts for the exclusive localisation of ENTPD3 CAR
366 Tregs to the pancreatic islets and not to the draining lymph nodes. Our findings show that
367 ENTPD3 CAR Tregs suppress immune responses through cross-suppression of CD4+ effector T
368 cells with diverse antigen specificities and a critical feature in T1D where autoimmune
369 responses target multiple beta cell antigens.

370 The concept of cross-suppression aligns with observations from transplantation models,
371 where CAR Tregs activated by HLA-A*02 locally controlled immune responses against
372 mismatched grafts with multiple allospecific T cells[15]. Moreover, a recent study by Levings et
373 al. demonstrated that local activation of CAR Tregs can lead to the conversion of beta cell
374 antigen-specific naïve T cells into Tregs[36], a phenomenon previously described as "infectious
375 tolerance" by Waldman et al[37].

376 Transcriptomic analyses revealed that ENTPD3 CAR Tregs share activation profiles with TCR-
377 activated Tregs, including upregulation of key regulatory genes such as IL-10, TGF-β, CTLA-4,
378 and CD25. Notably, ENTPD3 CAR Tregs also exhibited increased expression of inhibitory
379 receptors like LAG3, PD1, and TIGIT without signs of exhaustion[38].

380 Concerns regarding the potential cytotoxicity of CAR Tregs[39,40] were not observed in our
381 study. ENTPD3-positive target cells, including HEK and B cells, did not exhibit signs of
382 cytotoxicity following exposure to ENTPD3 CAR Tregs. This non-cytotoxic nature aligns with
383 observations of ENTPD3 CARs[40] and our in vivo data, where metabolic function remained
384 stable despite high local densities of ENTPD3 CAR Tregs in NOD islets.

385 Ensuring phenotypic stability of human Tregs is critical for minimising the risk of
386 differentiation into proinflammatory effector cells. By employing highly purified naïve Treg
387 populations (CD25high CD127- CD45RA+), we mitigated risks associated with less stable Treg
388 subsets[41,42]. ENTPD3 CAR Tregs exhibited stable demethylation in the Treg-specific
389 demethylated region (TSDR), further demonstrating their phenotype stability[26].

390 Future enhancements of phenotype stability could include incorporating FOXP3 transgenes
391 into the CAR construct to bolster Treg stability and suppressor function under inflammatory
392 conditions[43,44] or strengthening the STAT5 signalling[45].

393 Alternative beta cell-specific CAR targets, such as insulin and tetraspanin 7[17,23], have been
394 explored, but none have demonstrated comparable efficacy. ENTPD3 CAR Tregs offer a more
395 versatile and non-MHC-restricted approach, paving the way for local immune control in T1D.

396 Our findings represent a significant advancement in the clinical translation of ENTPD3 CAR
397 Tregs for T1D therapy. This approach could support endogenous beta cell regeneration in early
398 T1D stages or complement transplantation of islets or stem-cell derived beta cells in advanced
399 disease stages, potentially reducing reliance on systemic immunosuppression. ENTPD3 CAR
400 Tregs hold promise as a "living drug" capable of achieving sustained, local immune regulation,
401 representing a novel and transformative therapeutic option in the treatment of T1D.

Acknowledgements (186 words)

This work was supported by the ReSHAPE program, funded under the EU2020 program, with additional support from The Leona M. and Harry B. Helmsley Charitable Trust (2018PG-T1D06.3) and JDRF (3-SRA-2024-1529-S-B). Human CAR characterization was done in collaboration with Quell Therapeutics and Astra Zeneca. Quell Therapeutics supported the work at MHH as part of collaborative research support. Experiments with reaggregated human pseudoislets were done in collaboration with Quell Therapeutics and InSphero AG. This research was performed with the support of the Network for Pancreatic Organ Donors with Diabetes (nPOD), a collaborative type 1 diabetes research project funded by JDRF. Organ Procurement Organizations partnering with nPOD to provide research resources are listed at www.jdrfnpod.org/our-partners.php. The authors want to express their thank to Matthias Ballmaier of MHH's Central Research Facility Cell Sorting for supervision and support. Maximilian Fuchs of Fraunhofer Institute for Toxicology and Experimental Medicine (ITEM) for providing help in RNAseq data interpretation and to the Hannover Biomedical Research School (HBRS) for attending the PhD project of Tom Pieper. The PhD thesis of Tom Pieper and Master thesis of Viktor Glaser contains parts of the data published here.

Conflict of interest

TP, TR, MHW, MH and EJ are inventors of patent application on antibodies against ENTPD3 and the corresponding CAR-Tregs. EJ is shareholder of Quell Therapeutics. JMcG, TL, MML, KB, LH, DP, AG, TG, EN, ND, VK, PC are officers of Quell Therapeutics and LD, LJ, BZ, MS, JP, IM are officers of Astra Zeneca.

425 **References**

426 1. Lind, M.*, et al.* Glycemic control and excess mortality in type 1 diabetes. *N Engl J Med*
427 **371**, 1972-1982 (2014).
428 2. Beck, R.W.*, et al.* The T1D Exchange clinic registry. *J Clin Endocrinol Metab* **97**, 4383-
429 4389 (2012).
430 3. Rawshani, A.*, et al.* Mortality and Cardiovascular Disease in Type 1 and Type 2
431 Diabetes. *N Engl J Med* **376**, 1407-1418 (2017).
432 4. Wadwa, R.P.*, et al.* Trial of Hybrid Closed-Loop Control in Young Children with Type 1
433 Diabetes. *N Engl J Med* **388**, 991-1001 (2023).
434 5. Choudhary, P.*, et al.* Advanced hybrid closed loop therapy versus conventional
435 treatment in adults with type 1 diabetes (ADAPT): a randomised controlled study.
436 *Lancet Diabetes Endocrinol* **10**, 720-731 (2022).
437 6. Reichman, T.*, et al.* Glucose-dependent insulin production and insulin-independence
438 in patients with type 1 diabetes infused with stem cell-derived, fully differentiated
439 islet cells (VX-880). in *EASD*, Vol. 66 (Suppl1) S229 (Diabetologia, Hamburg, 2023).
440 7. Herold, K.C.*, et al.* An Anti-CD3 Antibody, Teplizumab, in Relatives at Risk for Type 1
441 Diabetes. *N Engl J Med* **381**, 603-613 (2019).
442 8. Ramos, E.L.*, et al.* Teplizumab and beta-Cell Function in Newly Diagnosed Type 1
443 Diabetes. *N Engl J Med* **389**, 2151-2161 (2023).
444 9. Bluestone, J.A.*, et al.* Type 1 diabetes immunotherapy using polyclonal regulatory T
445 cells. *Science translational medicine* **7**, 315ra189 (2015).
446 10. Marek-Trzonkowska, N.*, et al.* Administration of CD4+CD25highCD127- regulatory T
447 cells preserves beta-cell function in type 1 diabetes in children. *Diabetes Care* **35**,
448 1817-1820 (2012).
449 11. Tang, Q.*, et al.* In Vitro-expanded Antigen-specific Regulatory T Cells Suppress
450 Autoimmune Diabetes. *J Exp Med* **199**, 1455-1465 (2004).
451 12. Tarbell, K.V., Yamazaki, S., Olson, K., Toy, P. & Steinman, R.M. CD25+ CD4+ T Cells,
452 Expanded with Dendritic Cells Presenting a Single Autoantigenic Peptide, Suppress
453 Autoimmune Diabetes. *J Exp Med* **199**, 1467-1477 (2004).
454 13. Jaeckel, E., von Boehmer, H. & Manns, M.P. Antigen-Specific FoxP3-Transduced T-Cells
455 Can Control Established Type 1 Diabetes. *Diabetes* **54**, 306-310 (2005).
456 14. MacDonald, K.G.*, et al.* Alloantigen-specific regulatory T cells generated with a
457 chimeric antigen receptor. *J Clin Invest* **126**, 1413-1424 (2016).
458 15. Noyan, F.*, et al.* Prevention of Allograft Rejection by Use of Regulatory T Cells With an
459 MHC-Specific Chimeric Antigen Receptor. *Am J Transplant* **17**, 917-930 (2017).
460 16. Boardman, D.A.*, et al.* Expression of a Chimeric Antigen Receptor Specific for Donor
461 HLA Class I Enhances the Potency of Human Regulatory T Cells in Preventing Human
462 Skin Transplant Rejection. *Am J Transplant* **17**, 931-943 (2017).
463 17. Tenspolde, M.*, et al.* Regulatory T cells engineered with a novel insulin-specific
464 chimeric antigen receptor as a candidate immunotherapy for type 1 diabetes. *J*
465 *Autoimmun* **103**, 102289 (2019).
466 18. Docherty, F.M.*, et al.* ENTPD3 Marks Mature Stem Cell-Derived beta-Cells Formed by
467 Self-Aggregation In Vitro. *Diabetes* **70**, 2554-2567 (2021).
468 19. Syed, S.K.*, et al.* Ectonucleotidase NTPDase3 is abundant in pancreatic beta-cells and
469 regulates glucose-induced insulin secretion. *Am J Physiol Endocrinol Metab* **305**,
470 E1319-1326 (2013).

471 20. Saunders, D.C., *et al.* Ectonucleoside Triphosphate Diphosphohydrolase-3 Antibody
472 Targets Adult Human Pancreatic beta Cells for In Vitro and In Vivo Analysis. *Cell*
473 *Metab* **29**, 745-754 e744 (2019).
474 21. Fasolino, M., *et al.* Single-cell multi-omics analysis of human pancreatic islets reveals
475 novel cellular states in type 1 diabetes. *Nat Metab* **4**, 284-299 (2022).
476 22. Posey, A.D., Jr., Young, R.M. & June, C.H. Future perspectives on engineered T cells for
477 cancer. *Trends Cancer* **10**, 687-695 (2024).
478 23. Pieper, T., *et al.* Generation of Chimeric Antigen Receptors against Tetraspanin 7. *Cells*
479 **12**(2023).
480 24. Lavoie, E.G., *et al.* Identification of the ectonucleotidases expressed in mouse, rat,
481 and human Langerhans islets: potential role of NTPDase3 in insulin secretion. *Am J*
482 *Physiol Endocrinol Metab* **299**, E647-656 (2010).
483 25. Dawson, N.A.J., *et al.* Functional effects of chimeric antigen receptor co-receptor
484 signaling domains in human regulatory T cells. *Science translational medicine*
485 **12**(2020).
486 26. Polansky, J.K., *et al.* DNA methylation controls Foxp3 gene expression. *Eur J Immunol*
487 **38**, 1654-1663 (2008).
488 27. Hamieh, M., Mansilla-Soto, J., Riviere, I. & Sadelain, M. Programming CAR T Cell
489 Tumor Recognition: Tuned Antigen Sensing and Logic Gating. *Cancer discovery* **13**,
490 829-843 (2023).
491 28. Yesildag, B., *et al.* Liraglutide protects beta-cells in novel human islet spheroid models
492 of type 1 diabetes. *Clin Immunol* **244**, 109118 (2022).
493 29. Skowera, A., *et al.* beta-cell-specific CD8 T cell phenotype in type 1 diabetes reflects
494 chronic autoantigen exposure. *Diabetes* **64**, 916-925 (2015).
495 30. Sawitzki, B., *et al.* Regulatory cell therapy in kidney transplantation (The ONE Study):
496 a harmonised design and analysis of seven non-randomised, single-arm, phase 1/2A
497 trials. *Lancet* **395**, 1627-1639 (2020).
498 31. Serr, I., *et al.* Type 1 diabetes vaccine candidates promote human Foxp3(+)Treg
499 induction in humanized mice. *Nat Commun* **7**, 10991 (2016).
500 32. De Paula Pohl, A., *et al.* Engineered regulatory T cells expressing myelin-specific
501 chimeric antigen receptors suppress EAE progression. *Cell Immunol* **358**, 104222
502 (2020).
503 33. Yoon, J., *et al.* FVIII-specific human chimeric antigen receptor T-regulatory cells
504 suppress T- and B-cell responses to FVIII. *Blood* **129**, 238-245 (2017).
505 34. Ghilardi, G., *et al.* T cell lymphoma and secondary primary malignancy risk after
506 commercial CAR T cell therapy. *Nat Med* **30**, 984-989 (2024).
507 35. Bonifant, C.L., Jackson, H.J., Brentjens, R.J. & Curran, K.J. Toxicity and management in
508 CAR T-cell therapy. *Mol Ther Oncolytics* **3**, 16011 (2016).
509 36. Wardell, C.M., *et al.* Short Report: CAR Tregs mediate linked suppression and
510 infectious tolerance in islet transplantation. *bioRxiv* (2024).
511 37. Cobbold, S. & Waldmann, H. Infectious tolerance. *Curr Opin Immunol* **10**, 518-524
512 (1998).
513 38. Lamarche, C., *et al.* Tonic-signaling chimeric antigen receptors drive human regulatory
514 T cell exhaustion. *Proc Natl Acad Sci U S A* **120**, e2219086120 (2023).
515 39. Boroughs, A.C., *et al.* Chimeric antigen receptor costimulation domains modulate
516 human regulatory T cell function. *JCI Insight* **5**(2019).

40. Wu, X.*, et al.* CD39 delineates chimeric antigen receptor regulatory T cell subsets with distinct cytotoxic & regulatory functions against human islets. *Frontiers in immunology* **15**, 1415102 (2024).
41. Liu, W.*, et al.* CD127 expression inversely correlates with FoxP3 and suppressive function of human CD4+ T reg cells. *J Exp Med* **203**, 1701-1711 (2006).
42. Sakaguchi, S., Vignali, D.A., Rudensky, A.Y., Niec, R.E. & Waldmann, H. The plasticity and stability of regulatory T cells. *Nat Rev Immunol* **13**, 461-467 (2013).
43. McGovern, J., Holler, A., Thomas, S. & Stauss, H.J. Forced Fox-P3 expression can improve the safety and antigen-specific function of engineered regulatory T cells. *J Autoimmun* **132**, 102888 (2022).
44. Henschel, P.*, et al.* Supraphysiological FOXP3 expression in human CAR-Tregs results in improved stability, efficacy, and safety of CAR-Treg products for clinical application. *J Autoimmun* **138**, 103057 (2023).
45. Kremer, J.*, et al.* Membrane-bound IL-2 improves the expansion, survival, and phenotype of CAR Tregs and confers resistance to calcineurin inhibitors. *Frontiers in immunology* **13**, 1005582 (2022).